TITLE: Design of GaN/A1GaN HEMT Class-E Power Amplifier Considering Trapping and Thermal Effects

Design of GaN/AlGaN HEMT Class-E Power Amplifier Considering Trapping and Thermal Effects

Syed S. Islam and A. F. M. Anwar
Department of Electrical and Computer Engineering
University of Connecticut, Storrs, CT 06269-2157
Voice: (860) 486-3979, Fax: (860) 486-2447, Email: anwara@engr.uconn.edu

Abstract

A microwave class-E power amplifier using AlGaN/GaN HEMT as the switching device is reported by incorporating trapping and thermal effects in the large-signal device model. The load network of the class-E amplifier is designed by considering more realistic exponential decay of the drain current during fall time and finite quality factor of the resonant circuit to incorporate the nonidealities of the active device and passive components. With 9V supply voltage, calculated output power and power conversion efficiency are 89mW and 58% at 1GHz which decrease to 84mW and 54% at 3.8GHz, respectively for a $GaN/Al_{0.30}Ga_{0.70}N$ HEMT with gate width of 50μm.

Introduction

Class-E amplifiers [1-3] are suitable for nonlinear modulation schemes used by cellular and cordless standards like GSM and DECT and are popular for their higher power conversion efficiencies. Using GaAs MESFETs as the active device, Sowlati *et al.* [2] have reported a class-E amplifier with power added efficiency (PAE) of 50%, output power of 250mW at a supply voltage of 2.5 V at 835 MHz. Tsai *et al.* [3] have demonstrated operation of a class-E amplifier up to 1.9 GHz using 0.35 μm CMOS technology with PAE of 48% at a supply voltage of 2 V.

In recent years, GaN based HEMTs are pursued extensively for applications in high power microwave amplifiers operating at high temperature. GaN with a band gap of 3.4eV has a breakdown field of 2MV/cm. With SiC as the substrate, GaN offers an overall thermal conductivity of 4.5 W/cm-K allowing the devices to be operated at elevated temperatures as high as 750C reported by Daumiller *et al.* [4]. Eastman [5] has demonstrated an output power density of 11.7 W/mm at 10GHz with a 0.3μm × 100μm AlGaN/GaN HEMT. A low field mobility of 1500 $cm^2\ V^{-1}s^{-1}$ along with a saturation velocity of 3×10^7 cm/s allows the realization of high frequency devices as demonstrated by Lu *et al.* [6] where f_T = 101 GHz and f_{max} = 155 GHz have been reported with a 0.12μm ×100μm GaN/AlGaN HEMT. In

0-7803-7478/02/$17.00 © 2002 IEEE

class-E amplifiers, efficiency decreases at elevated frequencies due to the higher power loss in the active device that forces the driving transistor to operate at elevated temperatures. Due to superior power performances at elevated frequencies and temperatures, GaN based devices can be more suitable in class-E power amplifiers.

The superb performances of GaN based devices are hindered by the trapping effects [7]. The presence of traps in the buffer layer causes current collapse that may lead to DC to RF dispersion of transconductance and output resistance thereby degrading device performances at elevated frequencies requiring device models to incorporate the trapping effects for accurate analysis of RF/analog circuits [8]. In our previous effort [1], we have reported a GaN-based class-E amplifier operating up to 11GHz neglecting the trapping effects in the large-signal device model. In this paper, a class-E power amplifier using AlGaN/GaN HEMT as the switching device is reported for possible applications in microwave and wireless circuits by incorporating trapping effects in the large-signal device model.

Analysis

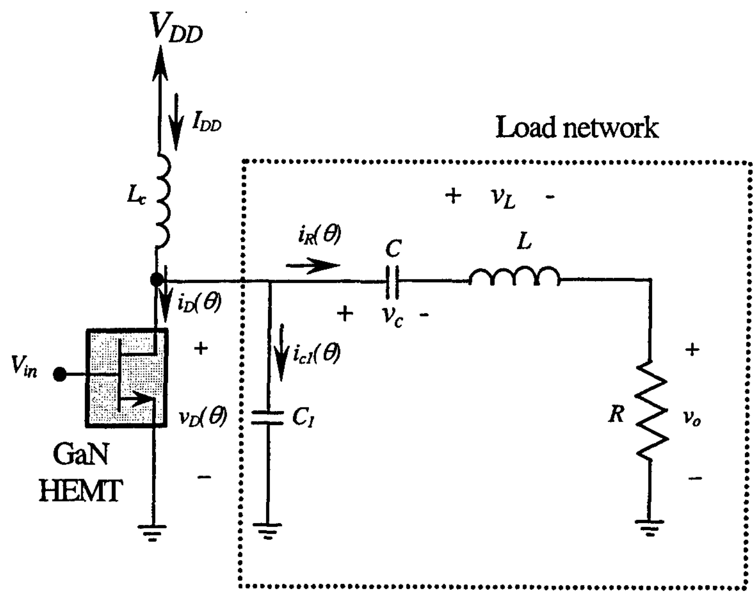

Fig.1. Basic class-E power amplifier circuit.

Fig.1 shows the basic class-E power amplifier circuit. The active device operates as a switch and the load network ensures minimum switching loss. A large-signal HEMT model, as shown in Fig.2, is used to realize the functional dependence of drain current upon applied gate and drain voltages. In Fig. 3, the dashed curve shows the measured *I-V* characteristics [7]. The negative slope of the modeled AC *I-V* characteristics, as shown in Fig. 3, is due to thermal effects. Surface traps located at the surface in the region between gate and drain were passivated by a layer of Si_3N_4. Current collapse and subsequent recovery at high drain bias have been correlated to the trapping and detrapping of carriers by the trapping centers located in the buffer layer [7]. Current collapse is dependent upon the applied signal frequency and causes the device transconductance and output resistance measured at DC to decrease significantly at RF [8]. Using drain-lag measurement data for AlGaN/GaN HEMTs, we have estimated detrapping time constants to be 58.42 seconds and 1.55 seconds that correspond to trap states located at 0.79eV and 0.69eV below the bottom of the conduction band, respectively. At room temperature, the transconductance and output resistance dispersion frequencies are less than 1Hz due to the trap levels mentioned above. However, with increasing temperature the dispersion frequencies increase and can be of the order of MHz at 600K. For applied signal frequencies greater than the output resistance and transconductance dispersion frequencies, traps are unable to respond and recovery of collapsed drain current is not possible. This necessitates the determination of the model parameters from the AC *I-V* characteristics as shown by the solid lines in Fig. 3. The AC drain current as function drain-source and gate-source voltages are given by,

$$I_{ds} = \left[f_o(V_{gs}) + f_1(V_{gs})V_{ds} + f_2(V_{gs})V_{ds}^2 + f_3(V_{gs})V_{ds}^3\right]\tanh\left[f_\alpha(V_{gs})V_{ds}\right] \tag{1}$$

where

$$f_\alpha(V_{gs}) = a_{\alpha o} + a_{\alpha 1}V_{gs} + a_{\alpha 2}V_{gs}^2 + a_{\alpha 3}V_{gs}^3, \tag{2}$$

$$f_i(V_{gs}) = a_{io} + a_{i1}V_{gs} + a_{i2}V_{gs}^2 + a_{i3}V_{gs}^3, \quad i = 0,\ldots,3, \tag{3}$$

the constants a's are given in Table 1. The intrinsic model parameters are given by,

$$g_m = \left.\frac{\partial I_{ds}}{\partial V_{gs}}\right|_{V_{ds}} \tag{4}$$

$$g_{ds} = \left.\frac{\partial I_{ds}}{\partial V_{ds}}\right|_{V_{gs}} \tag{5}$$

$$C_{gs,gd} = C_{gs0,gd0}\left(1 - \frac{V_{gs,gd}}{V_{bi}}\right)^{-\frac{1}{2}} \tag{6}$$

where, $C_{gs0,\ gd0}$ are zero-bias gate-source and gate-drain capacitances and V_{bi} is the built-in potential. The rest of the model parameters are obtained from reported experimental data [9,10] that are listed in Fig.2.

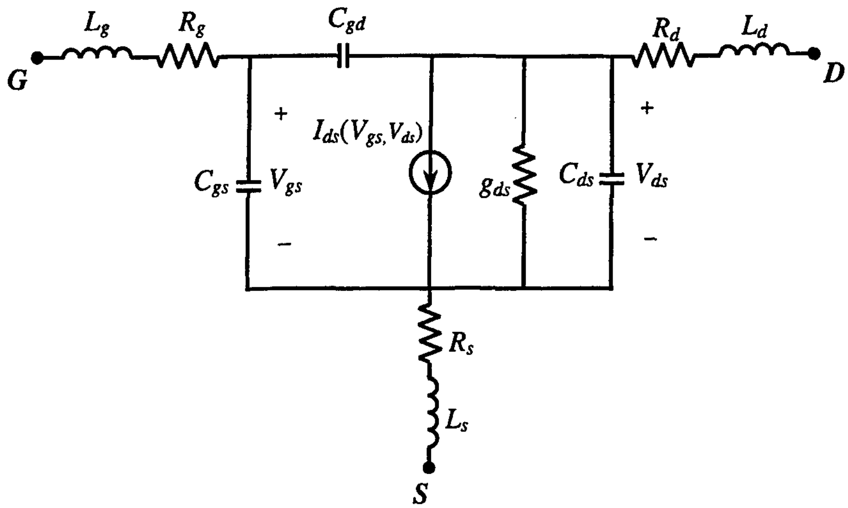

R_g	L_g	R_s	L_s	C_{ds}	R_d	L_d
0.5 Ω	0.09 nH	0.7 Ω	0.1 nH	0.44 pF/mm	0.5 Ω	0.07 nH

Fig.2. Equivalent circuit model of the GaN HEMT.

Table 1: Coefficients used in eqns. (2) - (3) defining GaN/$Al_{0.30}Ga_{0.70}N$ HEMT (width is 50μm, I_{ds} in milliamperes and V_{ds} and V_{gs} are in Volts) [7].

i	a_{i0}	a_{i1}	a_{i2}	a_{i3}
0	72.75	53.25	15.61	1.89
1	−6.51	−6.44	−1.64	−0.08
2	0.34	0.26	0.01	−0.01
3	−0.006	−0.002	0.002	0.0006
α	0.236	−0.270	−0.185	−0.090

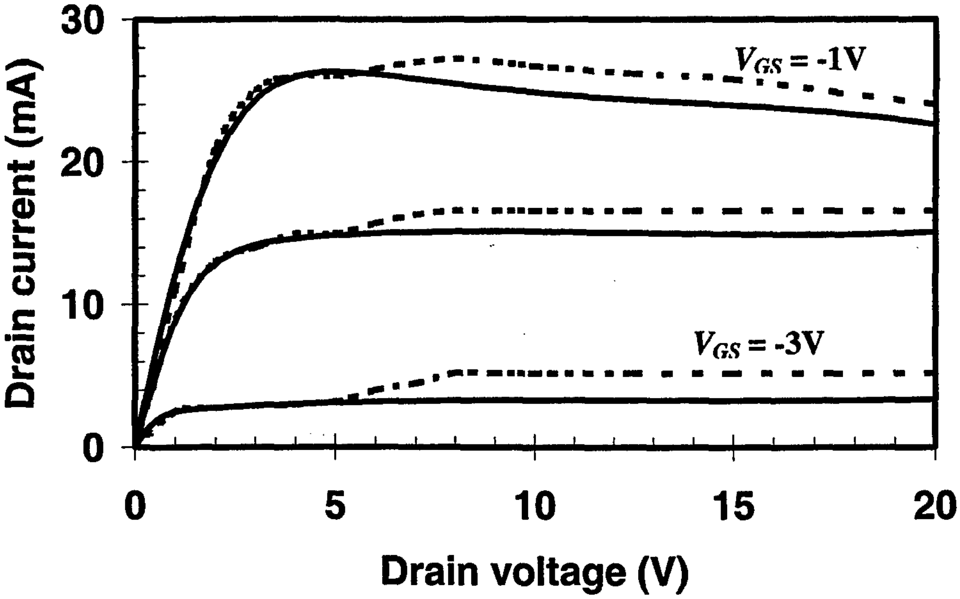

Fig.3. Simulated AC *I-V* characteristics of a GaN/AlGaN HEMT of 50μm gate width (solid lines). Experimental results are shown by dashed lines (DC *I-V*).

In the present analysis, the load network is designed by considering finite loaded quality factor of the inductor and exponential decay of the drain current during fall time. The load network components are as follows [1]:

$$C_1 = \frac{P_{out}\sin\phi\left[2+\frac{\pi^2}{2}+\pi\tan\phi+2\tau^2\left(1-e^{-\frac{t_f}{\tau}}\right)-2\tau\theta_f e^{-\frac{t_f}{\tau}}\right]^2}{2\pi\omega V_{dd}{}^2 k_1}, \tag{7}$$

$$R = \frac{k_1\sin\phi}{\pi\omega C_1}, \tag{8}$$

$$L = \frac{Q_L R}{\omega}, \tag{9}$$

and

$$C = \frac{1}{\omega^2\left(L-\frac{k_2\sin\phi}{\pi\omega^2 C_1}\right)}. \tag{10}$$

Here,

$$k_1 = \left[2\sin\phi + \cos\phi(4\omega\tau - \pi) - 2\cos\phi\cot\phi - 2\omega\tau e^{-\frac{t_f}{\tau}}\left\{\cos\phi + \cos(\theta_f + \phi)\right\} + \frac{2\omega^3\tau^3}{1+\omega^2\tau^2}\left\{\cos\phi - \cos(\theta_f + \phi)e^{-\frac{t_f}{\tau}} - \frac{1}{\omega\tau}\sin(\theta_f+\phi)e^{-\frac{t_f}{\tau}} + \frac{1}{\omega\tau}\sin\phi\right\}\right], \quad (11)$$

$$k_2 = \left[\frac{\pi}{2\sin\phi} - (4\omega\tau - \pi)\sin\phi - 2\omega\tau e^{-\frac{t_f}{\tau}}\left\{\sin\phi + \sin(\theta_f + \phi)\right\} + \frac{2\omega^3\tau^3}{1+\omega^2\tau^2}\left\{\sin\phi - \sin(\theta_f + \phi)e^{-\frac{t_f}{\tau}} + \frac{1}{\omega\tau}\cos(\theta_f+\phi)e^{-\frac{t_f}{\tau}} - \frac{1}{\omega\tau}\cos\phi\right\}\right], \quad (12)$$

$\theta_f = \omega\, t_f$ is the drain current fall angle, ϕ is the initial phase angle of the load current with respect to the load voltage at operating frequency ω, τ is the decay lifetime, P_{out} is the output power and Q_L is the loaded quality factor. ϕ is calculated by solving-

$$\frac{1}{\sin\phi} + \frac{\pi + \omega\tau\left(e^{-\frac{t_f}{\tau}} - 1\right)}{2\cos\phi + \omega\tau\sin\phi\left(e^{-\frac{t_f}{\tau}} - 1\right)} = 0, \quad (13)$$

which is obtained by applying the optimal switching conditions, namely, $v_D = 0$ and $dv_D(\omega t)/d(\omega t) = 0$ at $\omega t = 2\pi$ to the drain current and voltage equations.

Results and Discussion

The GaN/$Al_{0.30}Ga_{0.70}N$ HEMT reported by Binari *et al.* [7] is used to calculate the power and frequency performances of the class-E amplifier. The gate width is 50μm. The load network parameters are calculated considering a loaded quality factor of 10 and decay lifetime τ of the order of nanoseconds [1]. Fig.4 shows the calculated output power and efficiency of the class-E amplifier as a function of DC supply voltage at 3.8GHz that corresponds to the frequency at which peak pulsed power density of 6.7W/mm is reported [7]. Here, input signal has rectangular waveform which can be generated using a class-F driver [2]. As observed, with increasing DC supply voltage output power increases. Efficiency initially increases and eventually saturates due to the increase in DC power dissipation in the device. With a supply voltage of 9V, calculated output power of the class-E amplifier is 84mW and the power conversion efficiency is 54%. A similar variation in output power and efficiency was observed in the class-E power amplifier designed with GaAs MESFETs [2]. As GaN based devices are suitable for high voltage operation, higher output power can be obtained for given device dimensions using higher supply voltage. Besides, transient analysis shows that the drain voltage can be as high as 20V which can be sustained by the GaN HEMT without causing breakdown. As reported by Binari *et al.* [7], the application of a drain bias exceeding 20V caused current collapse in subsequent *I-V* measurements which necessities the incorporation of current collapse in the device model.

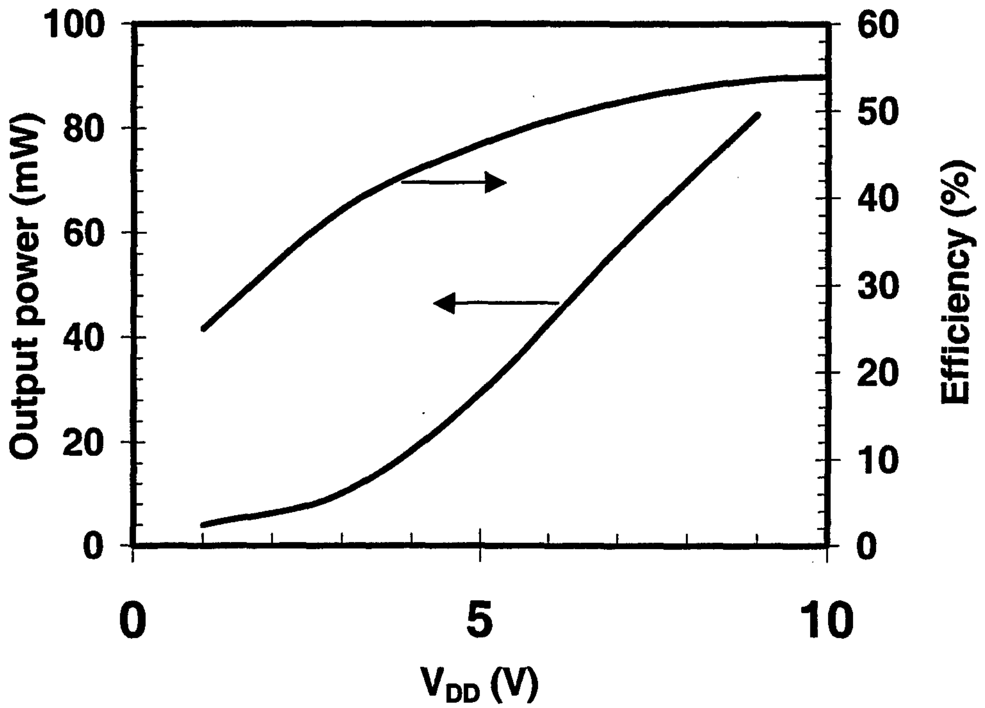

Fig.4. Calculated output power and efficiency as a function of DC supply voltage at 3.8GHz.

Output power and efficiency as a function of operating frequency are shown in Fig.5. Here supply voltage is 9V. At 1GHz, calculated efficiency and output power are 58% and 89mW, respectively. Output power and efficiency decrease monotonically with increasing frequency due to higher power loss at elevated frequencies [1].

To further investigate the effect of traps on the power performance of class-E amplifiers, simulations were carried out without accounting for current collapse in the device model. In the absence of current collapse, at 1GHz and with 9V supply voltage, output power increased to 114mW and efficiency increased to 60%. Similar results were obtained for output power and efficiency at elevated frequencies.

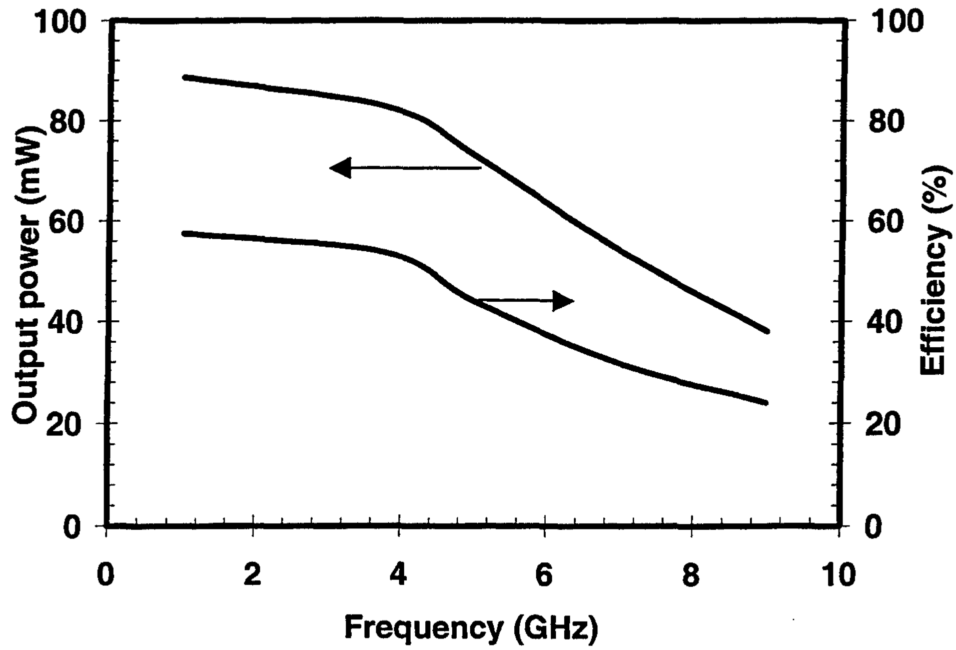

Fig.5. Calculated output power and efficiency as a function of frequency at 9V supply voltage.

Conclusions

A class-E power amplifier with AlGaN/GaN HEMT as the active device is reported. The large-signal model used in the simulation incorporates current collapse and DC to RF dispersions of transconductance and output resistance. A significant increase in operating frequency and efficiency of class-E power amplifier is obtained with GaN HEMT as the active device compared to that was reported with Si CMOS or GaAs MESFETs. Output power is significantly overestimated when current collapse is neglected in the device model.

References

[1] Syed S. Islam and A.F.M. Anwar, "GaN/AlGaN HEMT class-E power amplifier," To be published - *Solid-State Electron.*

[2] T. Sowlati, C.A. Salama, J. Sitch, G. Rabjohn and D. Smith, "Low voltage, high efficiency GaAs class-E power amplifiers for wireless transmitters," *IEEE J. of Solid-State Circuits*, Vol. 30, No. 10, pp.1074-1080, October 1995.

[3] King-Chun Tsai and P.R. Gray, "A 1.9 GHz 1-W CMOS Class-E power amplifier for wireless communications," *IEEE J. of Solid-State Circuits*, Vol. 34, No. 7, pp. 962-970, July 1999.

[4] I. Daumiller, C. Kirchner, M. Kamp, K.J. Ebeling, L. Pond, C.E. Weitzel and E. Kohn, "Evaluation of AlGaN/GaN HFETs up to 750 °C," *Device Research Conf. Dig.*, pp. 114-115, 1998.

[5] L.F. Eastman, "Experimental power-frequency limits of AlGaN/GaN HEMT's," *IEEE MTT-S Int. Microwave Symposium Dig.*, pp.2273-2275, June 2002.

[6] W. Lu, J. Yang. M.A. Khan and I. Adesida, "AlGaN/GaN HEMTs with over 100 GHz f_T and low microwave noise," *IEEE Trans. Electron Dev.*, Vol. 48, No. 3, pp. 581-585, March 2001.

[7] S.C. Binari, K. Ikossi, J.A. Roussos, W. Kruppa, D. Park, H.B. Dietrich, D.D. Koleske, A.E. Wickenden and R.L. Henry, "Trapping effects and microwave power performance in AlGaN/GaN HEMTs," *IEEE Trans. on Electron Devices*, Vol.48, No.3, pp. 465-477, March 2001.

[8] T. Ytterdal, T.A. Fjedly, M.S. Shur, S.M. Baier and R. Lucero, "Enhanced heterostructure field effect transistor CAD model suitable for simulation of mixed-mode circuits," *IEEE Trans. on Electron Dev.*, Vol. 46, No.8, pp. 1577-1588, August 1999.

[9] E. Alekseev, D. Pavlidis, N.X. Nguyen, C. Nguyen and D.E. Grider, "Power performance and scalibility of AlGaN/GaN power MODFETs," *IEEE Trans. on Microwave Theory and Tech.*, Vol. 48, No. 10, pp.1694-1700, October 2000.

[10] C-N Kuo, B.Houshmand and T. Itoh, "Full-wave analysis of packaged microwave circuits with active and nonlinear devices: an FDTD approach," *IEEE Trans. on Microwave Theory and Tech.*, Vol. 45, No. 5, pp.819-826, May 1997.